Rapid Communications

Picosecond time-resolved dynamics of energy transfer between GaN and the various excited states of Eu^{3+} ions

Ruoqiao Wei,[1] Brandon Mitchell,[2,3] Dolf Timmerman,[3] Tom Gregorkiewicz,[3,4] Wanxin Zhu,[3] Jun Tatebayashi,[3] Shuhei Ichikawa,[3] Yasufumi Fujiwara,[3] and Volkmar Dierolf[1]

[1]*Department of Physics, Lehigh University, Bethlehem, Pennsylvania 18015, USA*

[2]*Department of Physics, West Chester University, West Chester, Pennsylvania 19383, USA*

[3]*Division of Materials and Manufacturing Science, Graduate School of Engineering, Osaka University, 2-1 Yamadaoka, Suita, Osaka 565-0871, Japan*

[4]*Van der Waals-Zeeman Institute, University of Amsterdam, Science Park 904, 1098 XH Amsterdam, The Netherlands*

(Received 30 April 2019; revised manuscript received 17 July 2019; published 2 August 2019)

To elucidate the energy transfer and reexcitation processes in Eu-doped GaN layers that are used in recently developed, highly efficient red light-emitting diodes, a systematic series of photoluminescence and time-resolved photoluminescence (TR-PL) measurements was performed. Critical insights on how "slow" Eu processes (∼μs) can compete against fast semiconductor processes (∼ps) are revealed using TR-PL with a high temporal resolution, as it is found that the initial energy transfer from GaN to the Eu^{3+} ions takes place rapidly, on a timescale of <100 ps. Below band-gap resonant excitation was used to identify the states into which the energy transfer occurs. For the most efficient Eu defect complexes, this transfer dominantly occurs directly into the $^5D_0$ state of Eu^{3+}. Less efficient complexes also exhibit transfer into the $^5D_2$ state, the emission of which can be detected using photoluminescence at low temperature, indicating the importance of the excitation pathway on device efficiency. Under high excitation intensity, reexcitation can also occur, leading to a redistribution of population into the $^5D_2$, $^5D_1$, or $^5D_0$ states.

DOI: 10.1103/PhysRevB.100.081201

Artificial lighting is essential to modern society [1,2]. While incandescent lighting was dominant for decades, there has been a shift toward white solid-state light-emitting diodes (LEDs), which are becoming more accessible and more mainstream [3]. One aspect of white solid-state LEDs that is the subject of increasing attention is their reliance on high-intensity blue InGaN/GaN LEDs and a secondary excitation of phosphor mixtures to produce white light [4]. The blue light contribution in the spectrum of white LED bulbs and displays is significant and has been shown to disrupt human circadian rhythms [5]. Thus, methods for producing "warmer" LEDs, with a limited contribution of blue light, need to be investigated. One method is to utilize additive color mixing of red, green, and blue LEDs, instead of phosphor excitation, to produce white light. For this application, an efficient red emitter based on GaN is required.

Europium-doped GaN (GaN:Eu) is a good candidate for such red LEDs for two reasons: (1) Commercialized blue and green LEDs are both based on GaN and can be integrated with a GaN-based red LED [6]. (2) The spectral position of the Eu^{3+} emission at 622 nm is sharp and thermally stable [7,8]. Recently, green emission at ∼545 nm was observed in GaN:Eu devices due to transitions from higher excited states of the Eu^{3+} ions [9]. In addition, it was found that the emission spectrum of GaN:Eu could be modified under pulsed laser excitation or current injection, which offers an alternative avenue toward realizing warmer LEDs; however, the mechanism behind this phenomenon is not yet clear [9,10]. A better understanding of the energy transfer pathways from GaN to the Eu^{3+} ions, as well as the excited-state population dynamics within the Eu^{3+} energy-level manifold, will allow for an enhancement in the efficiency of Eu-doped GaN-based devices, further control over the emitted color from these devices, and potentially to the development of electrically pumped single photon emitters.

In this Rapid Communication, we present time-resolved photoluminescence results that detail the energy transfer and reexcitation dynamics of Eu^{3+} ions doped into GaN on the picosecond timescale. The results indicate that the initial energy transfer from the GaN host to the Eu^{3+} ions occurs on a timescale of <100 ps. This is faster than the decay lifetime found for the free carrier emission at 370 nm of ∼350 ps (Fig. S1 [11]), which explains how Eu emission can compete against other intrinsic radiative recombination centers in GaN. Figure 1(a) shows the excited states of Eu^{3+}, which sit at different positions within the band gap of GaN with respect to the energy levels of intrinsic defects such as gallium and nitrogen vacancies [8]. We show that the individual $^5D_0$, $^5D_1$, and $^5D_2$ states of the Eu^{3+} play distinctive roles in the excitation/reexcitation process, which are influenced by local defect environments around the Eu^{3+} ions. The timescale of the energy transfer, which is dependent on the transfer pathway, appears to be a determinant for which centers are excited most efficiently under current injection. Moreover, it is shown that the deexcitation of Eu^{3+} ions in the $^5D_0$ state back into the $^7F_0$ ground state, and their subsequent reexcitation, is the underlying mechanism behind the conversion between the red emission (622 nm) and green emission (545 nm) previously reported [9,10]. We present a comprehensive excitation model and compare the experimental results with simulations.

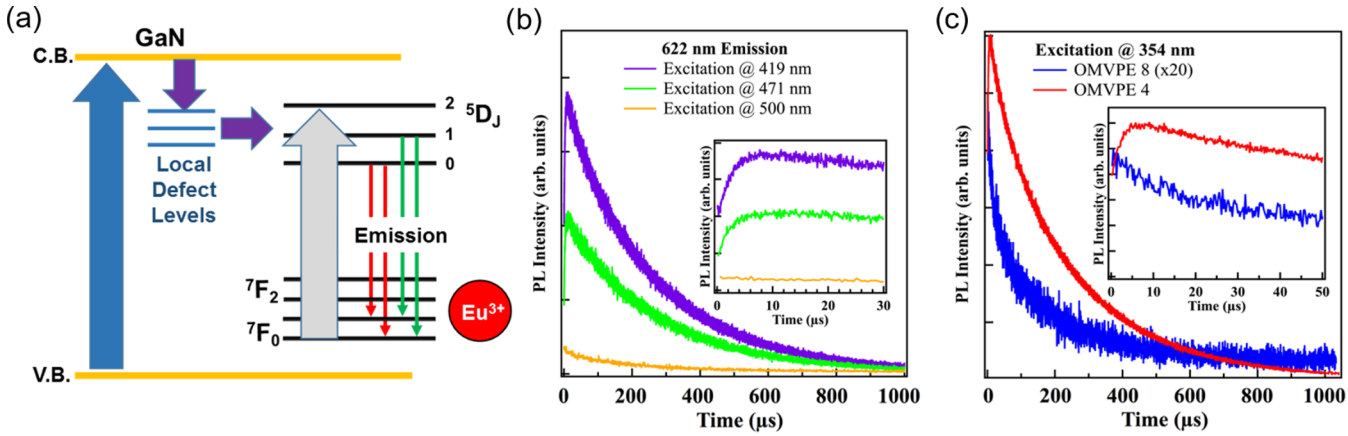

FIG. 1. (a) Energy-level scheme of the Eu^{3+} transitions observed in this study within the GaN band gap along with potential local defect trap levels. (b) TR-PL of $^5D_0$ state emission (622 nm) for excitation above the $^5D_2$ state, at the $^5D_2$ state, and in between the $^5D_2$ and $^5D_1$ states. (c) TR-PL on the OMVPE8 and OMVPE4 Eu centers under above band-gap excitation. The emission of OMVPE4 has a rise time while OMVPE8 does not.

To explore the temporal evolution of the excitation process, time-resolved photoluminescence (TR-PL) measurements were performed using an optical parametric oscillator (OPO) system (Solar LS). The third harmonic of a pulsed Nd:YAG laser (100 Hz, 5 ns pulse width) was used to pump a tunable OPO for generation of the different photon energies. Emission was dispersed by an M266 (Solar LS) monochromator coupled to a photomultiplier tube (Hamamatsu R928) combined with a multiscalar card, for photon detection. AlGaN/GaN:Eu multiple quantum well (MQW) samples consisting of 13 periods of alternating 10-nm $Al_xGa_{1-x}N$ layers and 3-nm GaN:Eu layers grown at 960 °C were chosen, as this sample structure was found to have a high-energy transfer efficiency [9,12]. (See Supplemental Material [11] for more details on the sample growth.)

Three excitation energies were chosen for the TR-PL measurements: (1) directly resonant with the $^5D_2$ state (471 nm), (2) above the $^5D_2$ state (419 nm), and (3) below the $^5D_2$ state, but above the $^5D_1$ state (500 nm). For all three excitation wavelengths, the emission was collected at 622 nm, and the result is shown in Fig. 1(b). When the excitation energy is higher than or resonant with the $^5D_2$ state, a rising component is observed in the emission from the $^5D_0$ state; however, this rise component is not observed when the excitation energy was in between the $^5D_2$ and $^5D_1$ states, and the emission intensity was significantly weaker. This is consistent with photoluminescence excitation (PLE) measurements, which revealed that the $^5D_2$ state exhibits a high absorption, indicating that it plays an important role in the initial excitation process; however, the $^5D_1$ state exhibits a significantly lower absorption, and does not [10]. The rise time was found to be $\sim 2\ \mu$s, which is on the same timescale as the lifetime of $^5D_1$ state. This indicates that the rising is due to a cascading relaxation from the $^5D_2 \rightarrow {}^5D_1 \rightarrow {}^5D_0$ state, and is consistent with previous reports [13,14]. These results confirm that the $^5D_0$ state can be excited via multiple pathways, which is influenced by the excitation energy with respect to the other ^5D_J states.

The Eu^{3+} ions have been shown to incorporate into GaN with diverse local defect environments or "sites" [15–22]. The results above indicate that the energy levels associated with these different defect environments can facilitate a preferential excitation of the Eu^{3+} ions into different ^5D_J states. "Site-selective" TR-PL was performed to elucidate this. The results are shown in Fig. 1(c). The 622-nm emission peak belongs *primarily* to the majority center in GaN:Eu, which is referred to as OMVPE4, at moderate excitation intensities [17–22]. The TR-PL results for OMVPE4 show a clear rise of $\sim 2\ \mu$s. For comparison, another Eu center referred to as OMVPE8 was selected as its primary emission peak ($\sim$618 nm) is easy to isolate from the other Eu emission peaks [20]. The TR-PL from OMVPE8 shows no rise under 354-nm excitation (above the GaN band gap), which confirms that the defect environment of the Eu^{3+} ion influences the energy transfer pathway.

To understand the dynamics behind this energy transfer mechanism on shorter timescales, TR-PL measurements were performed using a 342-nm PHAROS frequency tunable 200-fs pulse laser, and the emission was collected and sent to a Picoharp300 photon counting system with a temporal resolution of 512 ps. The repetition rate and pulse intensity of the laser were systematically varied to investigate the excitation and reexcitation properties of the different states of Eu^{3+}, and the influence of carrier density [9,10]. To study the behavior of Eu^{3+} ions in the ground state ($^7F_0$), the repetition rate was set to 1 kHz, resulting in a pulse interval longer than the lifetime of the $^5D_0$ state ($\sim 250\ \mu$s) [19]. On the other hand, the repetition rate was set to 200 kHz, resulting in a pulse interval much shorter than the lifetime of the $^5D_0$ state, allowing for the study of already excited Eu^{3+} ions in the presence of additional carriers.

Figure 2(a) shows the TR-PL results under a low pulse rate. With the enhanced time resolution of this detection system, it is clear that the Eu^{3+} ions are excited via two different pathways. One pathway is very fast where the $^5D_0$ state is directly populated. Using a low pulse intensity, it is shown that the $^5D_0$ state can be populated within 1 ns (inset). This process was not observed in the TR-PL results shown in Fig. 1, due to the lower temporal resolution of that system. The $^5D_0$ state is further populated via a different path ($\tau_{\text{rise}} \sim 2\ \mu$s) due to nonradiative decay from the $^5D_1$ state.

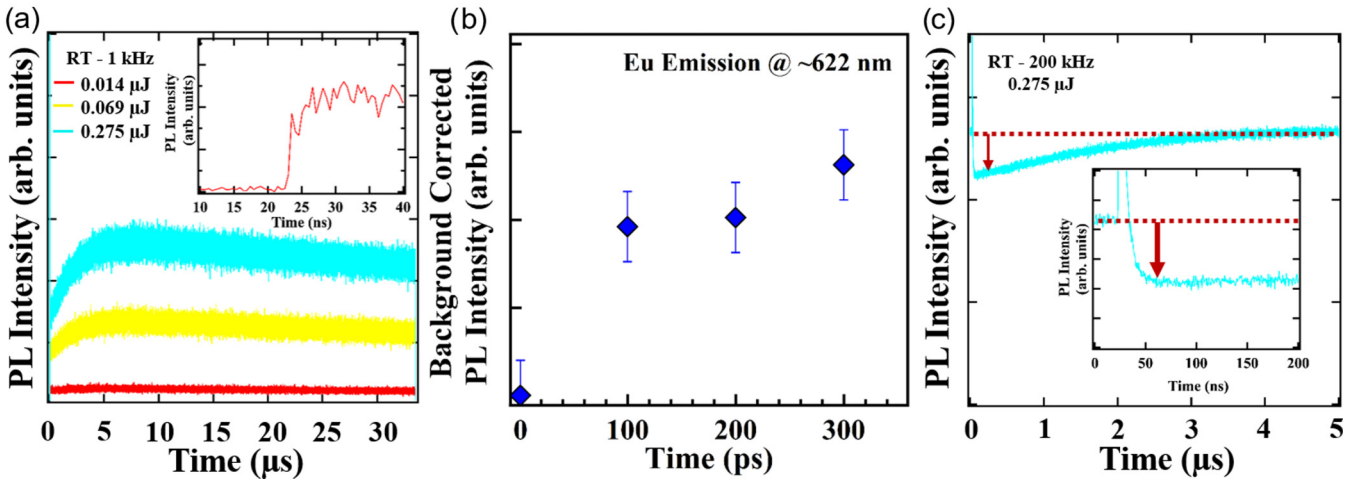

FIG. 2. (a) TR-PL at a repetition rate of 1 kHz measured at 622 nm and under different pulse intensities. Under low pulse intensity, $^5D_0$ related emission appears within 1 ns after the laser pulse (inset). (b) TR-PL emission using a streak camera at 100-ps binning and an intrinsic temporal resolution of 15 ps. Eu emission can be observed within 100 ps after the laser pulse. (c) TR-PL at a 200-kHz repetition rate under high pulse intensity. At this shorter pulse interval, the reexcitation processes can be observed.

As the pulse intensity was increased from 0.014 to 0.275 μJ, the ratio of the emission that went to the $^5D_0$ state directly compared to the relaxation-related emission decreased [Fig. 2(a)]. The difference in this ratio can be explained by the excitation of different Eu centers since, for the 622-nm peak, at least two centers (OMVPE4 and OMVPE7) overlap spectrally. (See Supplemental Material [11] for more details on the emission profiles from the different Eu centers, and how their emission can be spectrally selected.) OMVPE4 centers are numerous, but inefficient in terms of energy transfer, while the OMVPE7 centers are fewer in numbers and highly efficient [18,19]. Thus, the emission at 622 nm is dominated by OMVPE7 for very low pulse intensities, but saturates due to its low numbers. Furthermore, the emission under a pulse intensity of 0.014 μJ shows almost no slow rise component, which indicates that OMVPE7 is only excited through the fast pathway. Conversely, OMVPE4 emission can continue to increase due to its larger numbers, and the emission related to relaxation from the $^5D_1$ state increases proportionally. Spectrally resolved TR-PL on the 623-nm emission peak, which is only associated with OMVPE4, exhibits a constant proportionality between the fast and slow process (Fig. S4 [11]). This implies that the OMVPE4 centers can be excited through both the fast and slow pathways, with a certain branching ratio, while both OMVPE7 and OMVPE8 are only excited through the fast pathway. This observation is also consistent with a previous finding that these two centers are closely related [20].

Finally, still higher temporal resolution was needed to elucidate the fast energy transfer process; therefore, a streak camera (Hamamatsu C5680) was used. The sample was excited at 350 nm with an OPA Orpheus-HP (Light Conversion) pumped by a PHAROS femtosecond laser. Figure 2(b) shows background-corrected TR-PL on the 622-nm Eu emission, which can be observed within the first 100 ps after the laser pulse. (See Supplemental Material [11] for more details.) The high speed of the $^5D_0$ state population suggests that the energy transfer mechanism is an Auger-type process between the carriers and the electron configuration of the Eu^{3+} ions. A similar process was proposed for other rare-earth (RE) ions (Er and Yb) in Si [23–26]. Given the complicated $4f$ configuration of the RE ion, a quantitative estimate of transfer rates is extremely challenging. However, Auger processes in nitrides are, in general, very efficient and there is strong evidence for phonon-assisted Auger recombination in GaN, as predicted by first-principles theory [27,28]. Hence, we expect that such a process can be very efficient in our case as well.

Figure 2(c) shows TR-PL of the $^5D_0$ state emission under a high repetition rate (200 kHz). The $^5D_0$ emission intensity is reduced immediately after the pulse and then rises via relaxation from the $^5D_1$ state until the emission saturates. This is explained as a carrier-induced back-transfer [23,24], where a significant proportion of excited Eu^{3+} ions are deexcited out of the $^5D_0$ state, and the Eu^{3+} ions are excited again through a subsequent energy transfer. This result explains the shift in the relative ratio between the $^5D_1$ emission (545 nm) and the $^5D_0$ emission (622 nm) previously reported in GaN:Eu [9], however, it also demonstrates the short timescales at which excitation and reexcitation occur. This is shown with highest temporal resolution in Fig. S5 [11].

To gain a deeper understanding of the results above, a model of the reexcitation process was established using rate equations to simulate the energy transfer processes, as shown in Fig. 3(a). The energy levels considered in this model are the $^5D_2$, $^5D_1$, $^5D_0$, and ^7F_J (note: all ^7F levels are taken together). The transition from $^5D_2 \rightarrow {}^5D_1$ is a nonradiative decay, while the $^5D_0 \rightarrow {}^7F_J$ transitions are dominated by radiative decay. Clearly, the $^5D_1$ state can relax both radiatively and nonradiatively, since $^5D_1 \rightarrow {}^7F_J$ emission is observed in PL, and because the $^5D_0$ state emission increases due to decay from the $^5D_1$ state as observed in TR-PL. The pulse intensity (P) governs the excitation processes, and the pulse interval was set to 5 μs. The coefficients b, c, and d are branching ratio parameters for the different excitation and decay processes involved. Power-dependent photoluminescence results on the $^5D_1$ state emission revealed a linear relationship between PL

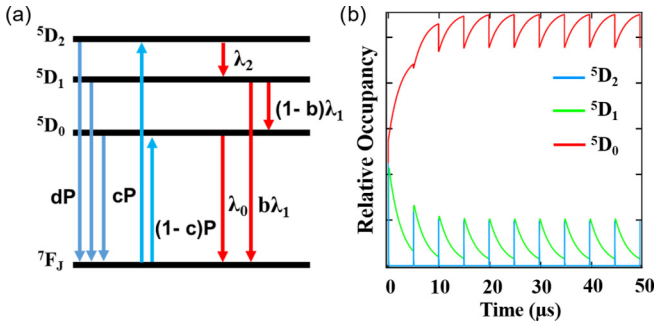

FIG. 3. (a) The Eu^{3+} energy levels and transitions used in the simulation. The dark blue arrows indicate back-transfer, the light blue arrows indicate excitation, and the red arrows represent the radiative and nonradiative transitions. (b) Simulation of the $^5D_0$, $^5D_1$, and $^5D_2$ state time evolution under high pulse intensity and high repetition rate.

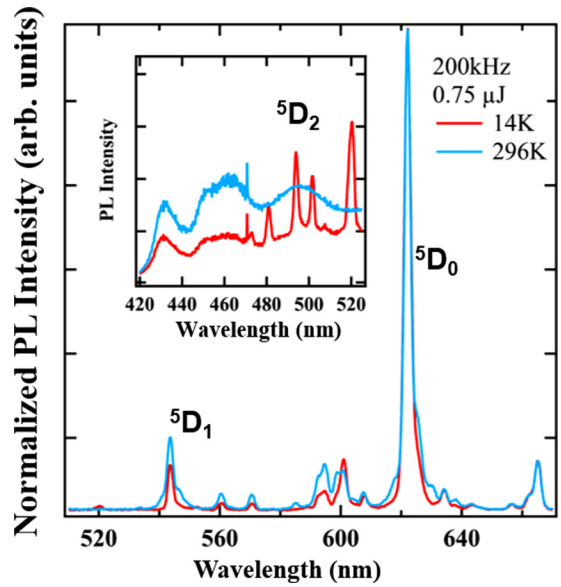

FIG. 4. PL at low temperature shows a relatively lower $^5D_1$ state emission compared with room temperature. In addition, $^5D_2$ emission can be detected at 472, 481, 494, 501, and 520 nm (inset) at low temperature, but not at room temperature.

emission intensity and pulse interval for all pulse energies, which indicates that the branching ratios are constant within the excitation parameters of these experiments (Fig. S7 [11]). The time evolution of the relative population of the $^5D_0$, $^5D_1$, and $^5D_2$ states is shown in Fig. 3(b). After five periods ($\sim$25 μs), the evolution results are consistent with the experimental TR-PL results shown in Fig. 2(b), where the $^5D_0$ state is depopulated after each pulse, and then subsequently repopulated both directly and via relaxation from the $^5D_1$ state. The $^5D_2$ state lifetime is sufficiently short such that no rise is observed in the $^5D_1$ state related emission, which is consistent within the 512-ps resolution of that measurement system. (The rate equations and details on the parameter determination can be found in the Supplemental Material [11].)

It is clear that nonradiative processes play an important role in the decay scheme from the $^5D_2$ state to the $^5D_0$ state [29,30]. To explore the role of these competitive nonradiative pathways, PL measurements were performed at low temperature ($\sim$14 K), where vibrations and nonradiative channels are inhibited. The samples were cooled using a closed-cycle He cryostat (Montana Instruments C_2 Cryostation) and the sample emission was collected using an OceanOptics USB4000 CCD spectrometer.

The PL emission spectra taken at 14 K and at room temperature are shown in Fig. 4, where the repetition rate of the pulses was set to 200 kHz. At low temperature, four new emission peaks are observed in the range of 470–520 nm (inset). The emission lines at 471, 480, 494, and 520 nm are related to transitions from the $^5D_2$ state to the $^7F_0$, $^7F_1$, $^7F_2$, and $^7F_3$ states, respectively. This observation confirms that the $^5D_2$ state can decay radiatively, but that it preferentially decays nonradiatively at room temperature; therefore, these peaks are absent in the room-temperature PL spectra. Moreover, no rise time was observed for the $^5D_2$ state emission, which suggests that energy transfer into the $^5D_2$ state also occurs on a timescale of $<$100 ps.

In summary, a detailed excitation model for GaN:Eu was established. We find that the initial energy transfer from the GaN to the Eu^{3+} ions occurs on a timescale of $<$100 ps, which is faster than the free-carrier luminescence in GaN at 370 nm with a decay lifetime of $\sim$350 ps. These results clarify how the "slow" processes within rare-earth atoms, which are known to interact weakly with their host environments, can compete against "fast" semiconductor processes leading to Eu-doped GaN-based red LEDs that can rival InGaN/GaN-based red LEDs in terms of external quantum efficiency. In addition, it is shown that energy is transferred to different ^5D_J states based on the local defect environment around the Eu^{3+} ion. This occurs because defect energy levels within the GaN band gap that are associated with these local defect environments are resonant with the energy levels of the different Eu^{3+} excited states (e.g., $^5D_2$, $^5D_1$, or $^5D_0$). For above band-gap excitation, the $^5D_0$ state of Eu^{3+} is populated with the highest probability relative to other Eu^{3+} states as there is a preference for all ^5D_J states to decay nonradiatively to the $^5D_0$ state by releasing phonons. It is proposed that the high efficiency of certain Eu centers (e.g., OMVPE7 and OMVPE8) results from a defect environment that primarily facilitates energy transfer directly into the $^5D_0$ state (fast pathway), whereas OMVPE4 is less efficient since it can be populated through either the slow or fast pathway.

Moreover, we show that Eu^{3+} ions in their long-lived $^5D_0$ state can be further excited, leading to an energy back-transfer to carriers (free or trapped) in the GaN host. The electron hole pairs subsequently recombine and transfer energy back to the Eu^{3+} ions, which redistributes to the $^5D_2$, $^5D_1$, and $^5D_0$ states according to their branching ratios. Multiple iterations of this reexcitation cycle can lead to a significant population of the $^5D_1$ state under intense excitation conditions. Interestingly, emission from the $^5D_2$ state can be observed at low temperatures, once nonradiative decay channels are inhibited. These results suggest that it should be possible to enhance the relative intensities of the $^5D_1$ and $^5D_2$ state-related emission by increasing the favorability of radiative decay.

Overall, the model and results give critical insights on the energy transfer efficiency in GaN:Eu. Blue InGaN/GaN-based LEDs have record-breaking external quantum efficiencies, despite an abundance of dislocations and defects, due to In phase decomposition, which creates a carrier localization effect, and the unique interaction between the In atoms and threading dislocations to form V- shaped pits that inhibit nonradiative recombination [31,32]. Similarly, the interaction between the Eu atoms and their local defect environment appears to be responsible for the unexpectedly high efficiencies of GaN:Eu-based devices. These results are essential for understanding how to manipulate the emission characteristics of the Eu^{3+} ions in order to facilitate color tunability in GaN devices, as well as the development of single photon emitting semiconductor systems based on Eu or other rare-earth elements.

The work at Lehigh University was supported by a CORE grant from Lehigh University. The work at Osaka University was partly supported by a Grant-in-Aid for Scientific Research (A) (JP17H01264) and a Grant-in-Aid for Specially Promoted Research (JP18H05212) from Japan Society for the Promotion of Science. B.M., Y.F., and T.G. thank Osaka University for the International Joint Research Promotion Program.

[1] M. Liu, B. Rong, and H. W. Salemink, Opt. Eng. **46**, 074002 (2007).
[2] M. G. Craford, Proc. SPIE **5941**, 594101 (2005).
[3] S. Pimputkar, J. S. Speck, S. P. DenBaars, and S. Nakamura, Nat. Photonics **3**, 180 (2009).
[4] J. K. Sheu, S. J. Chang, C. H. Kuo, Y. K. Su, W. Wu, Y. C. Lin, W. C. Lai, J. M. Tsai, G. C. Chi, and R. K. Wu, IEEE Photonics Technol. Lett. **15**, 18 (2003).
[5] K. M. Zielinska-Dabkowska, Nature (London) **553**, 274 (2018).
[6] P. Waltereit, O. Brandt, A. Trampert, H. T. Grahn, J. Menniger, M. Ramsteiner, M. Reiche, and K. H. Ploog, Nature (London) **406**, 865 (2000).
[7] H. Sekiguchi, Y. Takagi, T. Otani, R. Matsumura, H. Okada, and A. Wakahara, Jpn. J. Appl. Phys. **52**, 08JH01 (2013).
[8] B. Mitchell, V. Dierolf, T. Gregorkiewicz, and Y. Fujiwara, J. Appl. Phys. **123**, 160901 (2018).
[9] W. Zhu, R. Wei, D. Timmerman, T. Gregorkiewicz, B. Mitchell, Y. Fujiwara, and V. Dierolf, ACS Photonics **5**, 875 (2018).
[10] B. Mitchell, R. Wei, J. Takatsu, D. Timmerman, T. Gregorkiewicz, W. Zhu, S. Ichikawa, J. Tatebayashi, Y. Fujiwara, and V. Dierolf, ACS Photonics **6**, 1153 (2019).
[11] See Supplemental Material at http://link.aps.org/supplemental/10.1103/PhysRevB.100.081201 for additional data on the TR-PL for the GaN emission as well as a more detailed description of the rate equations and simulations.
[12] W. Zhu, B. Mitchell, D. Timmerman, A. Uedono, A. Koizumi, and Y. Fujiwara, APL Mater. **4**, 056103 (2016).
[13] H. Peng, C. W. Lee, H. O. Everitt, C. Munasinghe, D. S. Lee, and A. J. Steckl, J. Appl. Phys. **102**, 073520 (2007).
[14] L. Bodiou, A. Braud, J. L. Doualan, R. Moncorǵ, J. H. Park, C. Munasinghe, A. J. Steckl, K. Lorenz, E. Alves, and B. Daudin, J. Appl. Phys. **105**, 043104 (2009).
[15] Z. Fleischman, C. Munasinghe, A. J. Steckl, A. Wakahara, J. Zavada, and V. Dierolf, Appl. Phys. B **97**, 607 (2009).
[16] I. S. Roqan, K. P. O'Donnell, R. W. Martin, P. R. Edwards, S. F. Song, A. Vantomme, K. Lorenz, E. Alves, and M. Boćkowski, Phys. Rev. B **81**, 085209 (2010).
[17] N. Woodward, A. Nishikawa, Y. Fujiwara, and V. Dierolf, Opt. Mater. **33**, 1050 (2011).
[18] Y. Fujiwara and V. Dierolf, Jpn. J. Appl. Phys. **53**, 05FA13 (2014).
[19] R. Wakamatsu, D. G. Lee, A. Koizumi, V. Dierolf, Y. Terai, and Y. Fujiwara, Jpn. J. Appl. Phys. **52**, 08JM03 (2013).
[20] B. Mitchell, N. Hernandez, D. Lee, A. Koizumi, Y. Fujiwara, and V. Dierolf, Phys. Rev. B **96**, 064308 (2017).
[21] B. Mitchell, J. Poplawsky, D. Lee, A. Koizumi, Y. Fujiwara, and V. Dierolf, J. Appl. Phys. **115**, 204501 (2014).
[22] N. Woodward, J. Poplawsky, B. Mitchell, A. Nishikawa, Y. Fujiwara, and V. Dierolf, Appl. Phys. Lett. **98**, 011102 (2011).
[23] M. A. J. Klik, T. Gregorkiewicz, I. V. Bradley, and J.-P. R. Wells, Phys. Rev. Lett. **89**, 227401 (2002).
[24] M. Forcales, T. Gregorkiewicz, and M. S. Bresler, Phys. Rev. B **68**, 035213 (2003).
[25] W. Fuhs, I. Ulber, G. Weiser, M. S. Bresler, O. B. Gusev, A. N. Kuznetsov, V. Kh. Kudoyarova, E. I. Terukov, and I. N. Yassievich, Phys. Rev. B **56**, 9545 (1997).
[26] I. Yassievich, M. Bresler, and O. Gusev, J. Phys.: Condens. Matter **9**, 9415 (1977).
[27] M. Binder, A. Nirschl, R. Zeisel, T. Hager, H.-J. Lugauer, M. Sabathil, D. Bougeard, J. Wagner, and B. Galler, Appl. Phys. Lett. **103**, 071108 (2013).
[28] M. Brendel, A. Kruse, H. Jönen, L. Hoffmann, H. Bremers, U. Rossow, and A. Hangleiter, Appl. Phys. Lett. **99**, 031106 (2011).
[29] T. Andreev, N. Q. Liem, Y. Hori, M. Tanaka, O. Oda, D. L. S. Dang, and B. Daudin, Phys. Rev. B **73**, 195203 (2006).
[30] K. Binnemans, Coord. Chem. Rev. **295**, 1 (2015).
[31] K. P. O'Donnell, R. W. Martin, and P. G. Middleton, Phys. Rev. Lett. **82**, 237 (1999).
[32] A. Hangleiter, F. Hitzel, C. Netzel, D. Fuhrmann, U. Rossow, G. Ade, and P. Hinze, Phys. Rev. Lett. **95**, 127402 (2005).